Sparsity Sharing Embedding for Face Verification

Donghoon Lee, Hyunsin Park, Junyoung Chung,
Youngook Song, and Chang D. Yoo

Department of Electrical Engineering, KAIST, Daejeon, Korea

Abstract. Face verification in an uncontrolled environment is a challenging task due to the possibility of large variations in pose, illumination, expression, occlusion, age, scale, and misalignment. To account for these intra-personal settings, this paper proposes a sparsity sharing embedding (SSE) method for face verification that takes into account a pair of input faces under different settings. The proposed SSE method measures the distance between two input faces $\mathbf{x}_A$ and $\mathbf{x}_B$ under intra-personal settings s_A and s_B in two steps: 1) in the association step, $\mathbf{x}_A$ and $\mathbf{x}_B$ is represented in terms of a reconstructive weight vector and identity under settings s_A and s_B, respectively, from the generic identity dataset; 2) in the prediction step, the associated faces are replaced by embedding vectors that conserve their identity but are embedded to preserve the inter-personal structures of the intra-personal settings. Experiments on a MultiPIE dataset show that the SSE method performs better than the AP model in terms of the verification rate.

1 Introduction

In the past, many face verification algorithms have focused on determining discriminative face descriptors [12, 4, 9], optimal subspace learning [7, 6, 11, 13], and distance metric learning [10, 5]. Approaches using discriminative face descriptors have shown a good performance under a controlled environment, such as frontal face verification and by considering only illumination variations. However, the descriptors have a limitation in that variations due to changes in intra-personal settings are not always larger than variations due to changes in identity, as shown in Figure 1. Approaches based on optimal subspace learning and distance metric learning also find it difficult to handle uncontrolled environments, as a face space is considered as a non-linear manifold [7], and its capacity grows exponentially to cope with large intra-personal settings. Another difficulty is that non-rigid intra-personal variations involve 3D movement, e.g., pose changes, which cannot be modeled by linear transformations. Therefore, face verification in an uncontrolled environment remains a challenging problem.

To cope with large intra-personal variations, many recent approaches [20, 18, 1, 16, 8, 15, 17] have exploited prior knowledge for face verification. Wolf *et al.* [18] used a single positive sample and a set of background negative samples to train a binary classifier, and Blanz *et al.* [1] simulated the process of image formation in

Fig. 1. Variations due to change in intra-personal setting and identity. Histograms of Local Binary Patterns (LBP) are extracted from the faces, and Euclidean distances between the descriptors are illustrated.

3D space to estimate a 3D appearance transformation based on prior morphable 3D models. Su *et al.* [16] proposed an adaptive generic learning technique using a discriminant model based on an extra identity dataset. Kumar *et al.* [8] proposed an attribute simile classifiers, which characterize faces by high-level attributes and similes, and compared pairs of faces rather than the appearance of the face itself. The Doppelgänger list comparison proposed by Schroff *et al.* [15] also considered a large extra identity dataset. In this comparison method, two input faces are described by ordered lists of identities from the identity dataset, and the similarity between faces is determined by the lists. A face-sketch recognition idea proposed in [17] builds an identity dataset consisting of photo-sketch pairs. Input photos are reconstructed using a linear combination of the prior identity photos, and then a new sketch of the input photo is generated based on the prior photo-sketch pairs.

Yin *et al.* proposed the associate-predict (AP) model [20], which exploits prior knowledge to predict the probable face under different intra-personal settings. The AP model is built on a generic identity dataset where each identity contains multiple faces under large intra-personal settings. When two faces $\mathbf{x}_A$ and $\mathbf{x}_B$ under different intra-personal settings s_A and s_B are input, the AP model first associates $\mathbf{x}_A$ with the nearest face in the identity dataset. Using the associated face, $\mathbf{x}_A$ under s_B is predicted and this is used to either compare (appearance prediction) or discriminatively predict the likelihood of whether two faces belong to the same person (likelihood prediction).

This paper proposes a sparsity sharing embedding (SSE) method which incorporates the appearance prediction of the AP model for face verification. We employ the idea of using an identity dataset as a bridge to predict a face under different intra-personal settings. However, we also point out limitations of the AP model. This is its tendency to quantizes the associate space into the number of identities, leadings to the prediction space becoming quantized and causing an error between the prediction and ground truth that cannot be compensated. To resolve this problem, we consider two approaches in the association step: 1) K-NN association which minimizes the reconstruction error using K-nearest neighbors; 2) sparse association which minimizes the reconstruction error with

l_1 regularization. The reconstructive weights obtained from the association step cannot be shared over different intra-personal settings in the prediction step, because the structure of the identity set varies along the intra-personal setting. Therefore, in our method, associated identities are replaced with the embedding vectors that are pre-learned from the identity dataset to share the reconstructive weights of each intra-personal setting.

The rest of the paper is organized as follows. Section 2 reviews some related works, and Section 3 describes the details of the proposed method. We present experiments to evaluate the proposed method in Section 4, and discuss our conclusions in Section 5.

2 Association-prediction Approach for Face Verification

In this section, we briefly review the appearance prediction approach of the AP model. The AP model assumes that our brain adopts prior knowledge to verify the coincidence of the identities of two faces under different settings, takes a two-step approach (an association step and a prediction step) with the identity dataset. For example, our brain associates a new face with faces that we have seen before, and predicts a reasonable face under a different setting (for example, a prediction from a non-frontal face to its frontal version).

In the association step, given an input face $\mathbf{x}_A^{s_A} \in \mathbf{R}^d$, where the superscript indicates the estimated intra-personal setting, the AP model selects the most similar face based on the intra-personal setting, s_A, from the identity dataset $\mathcal{I} = \{\mathbf{x}_i^s \in \mathbf{R}^d | \ i = 1, \cdots, I \text{ and } s = 1, \cdots, S\}$ where I and S denote the number of identities and intra-personal settings, respectively. The association result can be described using reconstructive weight vector $\mathbf{w}_A \in \mathbf{R}^I$:

$$\begin{aligned} \mathbf{w}_A = \arg\min_{\mathbf{w}} ||\mathbf{x}_A^{s_A} - \sum_{i=1}^{I} w_i \mathbf{x}_i^{s_A}||_2^2 \\ \text{s.t.} \quad w_i \in \{0, 1\}, \\ \sum_i w_i = 1. \end{aligned} \tag{1}$$

For the other input face, $\mathbf{x}_B^{s_B}$, $\mathbf{w}_B$ can be obtained in the same way.

In the prediction step, the predicted face, $\tilde{\mathbf{x}}_A^{s_B}$, of identity A in setting s_B is obtained by

$$\tilde{\mathbf{x}}_A^{s_B} = \mathbf{X}^{s_B} \mathbf{w}_A, \tag{2}$$

where $\mathbf{X}^{s_B} = [\mathbf{x}_1^{s_B}, \cdots \mathbf{x}_I^{s_B}]$. $\tilde{\mathbf{x}}_B^{s_A}$ can also be obtained in a similar manner. As a result, the two inputted faces can be compared with the predicted faces in the same settings.

Finally, the distance between $\mathbf{x}_A^{s_A}$ and $\mathbf{x}_B^{s_B}$ are measured by considering the discriminative ability of each prediction using distance weights α_A and α_B:

$$d_p = \frac{1}{\alpha_A + \alpha_B}(\alpha_A d_A + \alpha_B d_B), \tag{3}$$

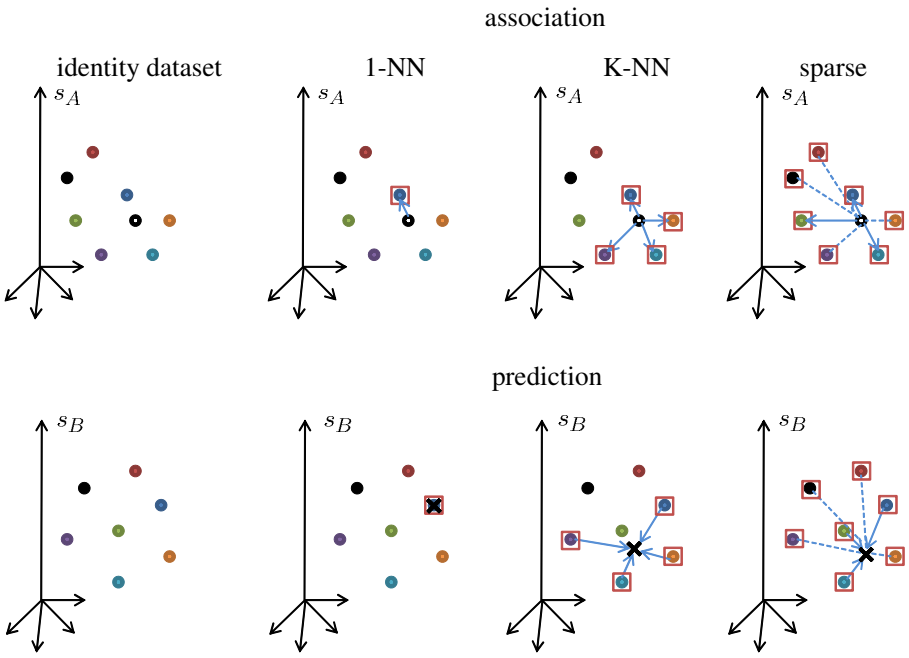

Fig. 2. Comparison between 1-NN, K-NN and sparse methods. Generic identities from the identity dataset $\mathbf{x}_i^{s_A}$ and $\mathbf{x}_i^{s_B}$ (filled-in circles), input face $\mathbf{x}_A^{s_A}$ (open circles), associated identities and reconstructive weights $\mathbf{w}_A$ (squares and lines), and prediction $\tilde{\mathbf{x}}_A^{s_B}$ (cross) are illustrated.

where $d_A = ||\tilde{\mathbf{x}}_A^{s_A} - \mathbf{x}_B^{s_A}||_2^2$ and $d_B = ||\tilde{\mathbf{x}}_B^{s_B} - \mathbf{x}_A^{s_B}||_2^2$ are the squared Euclidean distances. For the distance weights, $\alpha_A = e^{-\gamma||\tilde{\mathbf{x}}_A^{s_A} - \mathbf{x}_A^{s_A}||_2^2}$ and $\alpha_B = e^{-\gamma||\tilde{\mathbf{x}}_B^{s_B} - \mathbf{x}_B^{s_B}||_2^2}$ are used, and γ is a control parameter.

3 Sparsity Sharing Embedding

In this section, the details of the proposed SSE are described. To resolve the quantization problem of the AP model mentioned above, K-NN association and sparse association are both considered during the association step. In addition, we argue that the the reconstructive weights under different intra-personal settings are not consistent. To deal with this problem, embedding is employed to obtain the embedding vectors representing the identities to share the reconstructive weights from each intra-personal setting.

3.1 Association

Comparisons between 1-NN, K-NN and sparse association are summarized in Figure 2. In the 1-NN association, $\mathbf{x}_A^s$ is associated with the nearest identity in

the identity dataset. Hence, we can observe that the prediction space is quantized into only seven identities, and thus $\tilde{\mathbf{x}}_A^{s_B}$ can have only one of seven values (Figure 2).

K-NN Association In the K-NN association, $\mathbf{x}_A^s$ is associated with the K-NN identities by solving the following minimization problem:

$$\begin{aligned} \mathbf{w}_A = \arg\min_{\mathbf{w}} ||\mathbf{x}_A^{s_A} - \sum_i w_i \mathbf{x}_i^{s_A}||_2^2 \\ \text{s.t.} \quad w_i = 0, \text{ if } i \notin \mathcal{NN}_K(\mathbf{x}_A^{s_A}), \\ \sum_i w_i = 1. \end{aligned} \tag{4}$$

Here, $\mathbf{x}_i^{s_A}$ are the faces under setting s_A from $\mathcal{I}$, and $\mathcal{NN}_K(\mathbf{x}_A^{s_A})$ denotes the set of K-nearest neighbors of $\mathbf{x}_A^{s_A}$ among $\mathbf{x}_i^{s_A}$. In the above minimization problem, $\mathbf{x}_A^{s_A}$ is reconstructed using a linear combination of K-nearest neighborhoods and reconstructive weight vector $\mathbf{w}_A$, and we should try to find a value of $\mathbf{w}_A$ that minimizes the reconstruction error. The details about how to solve the above minimization problem is described in [14].

Sparse Association A sparse representation is used to code a data instance usng an over-complete dictionary and sparse reconstructive weight vector [19]. We adopt a sparse representation during the association step (sparse association). In a sparse association, input faces are associated with faces in the identity dataset using a sparse representation by solving the following minimization problem:

$$\mathbf{w}_A = \arg\min_{\mathbf{w}} ||\mathbf{x}^{s_A} - \sum_i w_i \mathbf{x}_i^{s_A}||_2^2 + \lambda||\mathbf{w}||_1 \tag{5}$$

where λ is the control parameter for l_1-regularization.

Compared to a K-NN association, a sparse association takes into account all faces in the identity dataset, but derives a small number of identities that are dominant for reconstruction of the input face with only the K-NN identities considered for reconstruction, as shown in Figure 2. We assume that the discriminative nature of the sparse representation [19] helps the sparse association perform better than the other association approaches described above.

3.2 Prediction using Embedding Vectors

To predict $\tilde{\mathbf{x}}_A^{s_B}$, reconstruction using reconstructive weight vector $\mathbf{w}_A$ and identities under intra-personal setting s_B can be considered. However, since the inter-personal structure (structure of the identities under the same intra-personal setting) of each intra-personal setting is inconsistent, as shown in Figure 4, using the reconstruction weights $\mathbf{w}_A$ in s_B can cause a significant prediction error.

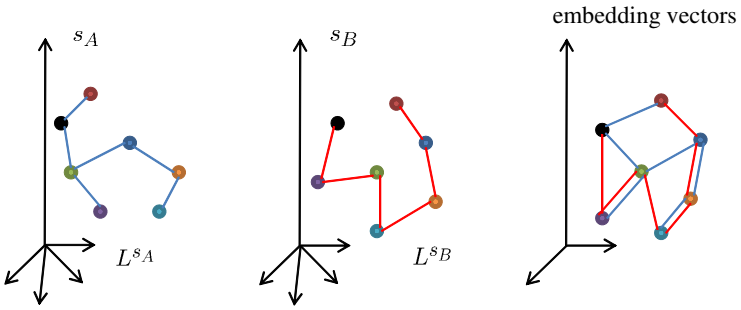

Fig. 3. Example of the SSE. Reconstructive weights from s_A and s_B are used to obtain the embedding vectors.

To resolve this problem, we adopted non-linear embedding to find embedding vectors $\mathbf{y}_1, \cdots, \mathbf{y}_I$ inter-personal structure of which considers the inter-personal structure of each intra-personal setting. Our embedding algorithm consists of two steps: 1) computing the inter-personal structure for each intra-personal settings, and 2) computing the embedding vectors that preserve the reconstructive weights from all intra-personal settings, as shown in Figure 3.

Computing the Inter-personal Structure. We define an inter-personal structure as a reconstructive weight matrix among the identities obtained using Equations (4) and (5). For K-NN, the inter-personal structure of setting s is computed by solving the following minimization problem:

$$\begin{aligned} \mathbf{L}^s = \arg\min_{\mathbf{L}} & \sum_{i=1}^{I} ||\mathbf{x}_i^s - \sum_{j \neq i} L_{ij}^s \mathbf{x}_j^s||_2^2 \\ \text{s.t.} \quad & L_{ij}^s = 0, \text{ if } j \notin \mathcal{NN}_K(\mathbf{x}_i^s), \\ & \sum_{j \neq i} L_{ij}^s = 1, L_{ii}^s = 0 \text{ for } i = 1, \cdots, I \end{aligned} \tag{6}$$

For a sparse representation, similar with K-NN, the inter-personal structures are computed by solving the following minimization problem.

$$\begin{aligned} \mathbf{L}^s = \arg\min_{\mathbf{L}} & \sum_{i=1}^{I} \left(||\mathbf{x}_i^s - \sum_{j \neq i} L_{ij}^s \mathbf{x}_j^s||_2^2 + \lambda ||\mathbf{L}_i^s||_1 \right) \\ \text{s.t.} \quad & L_{ii} = 0 \text{ for } i = 1, \cdots, I \end{aligned} \tag{7}$$

Note that the above inter-personal structures are similar with the adjacency matrix used in [6, 13] and can be obtained using the same way used in Equations (5) and (6).

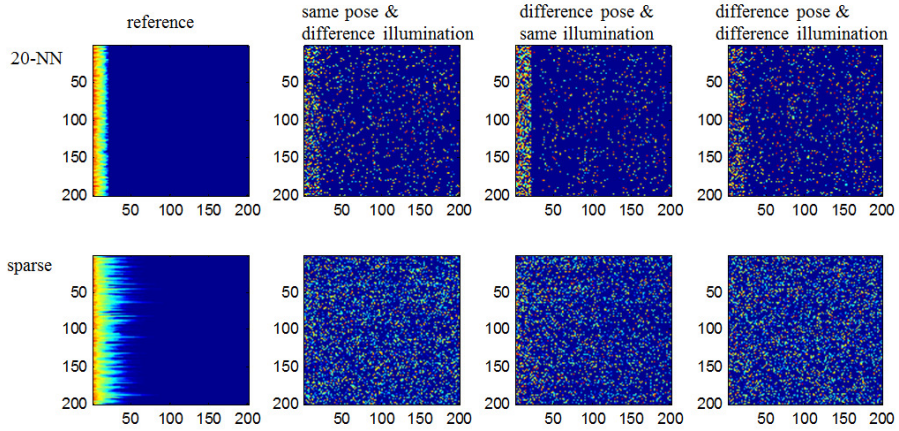

Fig. 4. Inter-personal structures of the identity dataset under various intra-personal settings are illustrated. Inter-personal structures are calculated using Equations (6) (top, 20-NN) and (7) (bottom, sparse). For visualization, row-wise indices (reconstructive weight vectors) are sorted in descending order based on the reference intra-personal setting (left), and the sorted indices are used to illustrate other local structures.

Computing Embedding Vectors. To compute the embedding vectors that preserve the reconstructive weights over all intra-personal settings, the following cost function, which averages the reconstruction errors over all settings, is considered.

$$\begin{aligned} \Phi(\mathbf{Y}) &= \frac{1}{S}\sum_{s=1}^{S}\Phi(\mathbf{Y},s) \\ &= \frac{1}{S}\sum_{s=1}^{S}\sum_{i=1}^{I}||\mathbf{y}_i - \sum_{j\neq i} L_{ij}^{s}\mathbf{y}_j||_2^2 \end{aligned} \tag{8}$$

Here, $\mathbf{y}_1, \cdots, \mathbf{y}_I$ are p-dimensional embedding vectors representing the identity $1, \cdots, I$, respectively, and $\mathbf{Y} = [\mathbf{y}_1, \cdots, \mathbf{y}_I]$. The solution that minimizes Equation (8), with the constraint $\mathbf{Y}\mathbf{Y}^T = \mathbf{I}$ used to avoid a degenerate problem, can be obtained by computing the $p+1$ eigenvectors corresponding to the smallest $p+1$ eigenvalues of the matrix $\mathbf{M} = \frac{1}{S}\sum_{s=1}^{S}(\mathbf{I}-\mathbf{L}^s)^T(\mathbf{I}-\mathbf{L}^s)$ and discarding the smallest eigenvalue [14]. Here, $\mathbf{I}$ denotes the identity matrix.

Prediction A prediction is made using the embedding vectors and reconstructive weight vector:

$$\begin{aligned} \tilde{\mathbf{y}}_A &= \mathbf{Y}\mathbf{w}_A \\ \tilde{\mathbf{y}}_B &= \mathbf{Y}\mathbf{w}_B. \end{aligned} \tag{9}$$

.

Fig. 5. Example faces of the MultiPIE dataset with seven pose variations under four illumination conditions.

An RBF kernel SVM [3] is adopted as a classifier using the concatenation of the element-wise absolute difference of predictions, $|\tilde{\mathbf{y}}_A - \tilde{\mathbf{y}}_B|$, and Hadamard product of predictions, $\tilde{\mathbf{y}}_A \circ \tilde{\mathbf{y}}_B$, as inputs.

4 Evaluation

We conducted experiments on the MultiPIE benchmark dataset to demonstrate the verification performance of each method (e.g., association and embedding methods) considered in the previous sections.

4.1 MultiPIE dataset

The MultiPIE dataset contains more than 750,000 faces from 337 identities, with 15 varying view points, 19 illumination conditions, and 4 different facial expressions. To build the identity dataset, we employed 319 identities collected from sessions 1 and 4 with using seven different poses under four illumination conditions, as shown in Figure 5. The poses used in our generic identity dataset range from $-45°$ to $45°$ with $15°$ intervals to cover the horizontal rotation. Among the 19 illumination conditions, which were obtained from 18 different flash directions and no flash, we used a left flash, frontal flash, right flash, and no flash. Two-hundred identities were considered as the generic identity dataset, and ten folders were randomly generated from the remaining 119 identities. Note that the identities in each folder are mutually exclusive. For each of the folders, 300 positive pairs and 300 negative pairs were randomly generated. The face

Table 1. Face verification results using K-NN association without embedding. Mean accuracies and standard deviations are represented in terms of %.

Descriptor	Direct	$K = 1$	$K = 5$	$K = 10$	$K = 20$	$K = 50$
SIFT	83.62±1.34	83.87±1.90	87.55±2.01	88.72±2.34	89.00±1.81	88.07±2.79
HOG	83.43±2.91	81.63±3.06	86.23±2.19	86.50±2.81	86.73±2.72	85.02±2.16
LBP	90.00±0.85	87.58±2.97	91.68±2.24	92.28±2.14	92.70±2.74	91.52±2.03

Table 2. Face verification results using K-NN association with embedding ($p = 50$). Mean accuracies and standard deviations are represented in terms of %.

Descriptor	Direct	$K = 1$	$K = 5$	$K = 10$	$K = 20$	$K = 50$
SIFT	83.62±1.34	74.67±2.23	85.55±2.32	86.00±2.16	84.73±1.72	82.78±3.25
HOG	83.43±2.91	82.85±2.32	90.72±1.63	91.73±1.81	92.67±2.07	91.77±3.14
LBP	90.00±0.85	85.75±3.38	92.85±2.20	93.82±1.94	93.67±2.38	92.08±2.54

verification performances were evaluated through a ten-fold cross validation, and the mean accuracies with standard deviations were reported for each method.

4.2 Face Representation & Intra-personal Setting Estimation

A facial component-level association was adopted following the method introduced in [20]. First, we generated nine patches containing facial components based on nine facial landmarks obtained using two-level cascaded regression [2]. Second, we extracted three types of low-level descriptors to represent the face images in our experiments: LBP [12], HOG [4], and SIFT [9].

For LBP, we used eight uniformly spaced circular neighbor sets with 58-code encoding. For SIFT, SIFT descriptors from three different scales at the nine landmarks were extracted. For HOG, we used 32 bins for quantization. Histogram-based descriptors (LBP and HOG) were extracted from a 3×3 division of each patch and concatenated. The low-level descriptors obtained were too large compared to the number of training samples; therefore, we applied PCA to the training set to reduce the dimensionality to 100.

In [20], Yin *et al.* pointed out that using a switching mechanism with direct matching of the feature vectors with similar settings drastically improves the verification performance. Our switching criteria differ slightly from those in [20]. Face prediction was applied to every pair that does not have the same setting. Intra-personal settings were estimated using the extracted feature vectors and an RFB kernel SVM [3].

4.3 Face Verification Experiments on the MultiPIE

Association Comparison For the final distance, d_p, in Equation (3), we strictly followed the set-up described in [20] except the distances, d_A and d_B,

Table 3. Face verification results using K-NN association with embedding ($p = 100$). Mean accuracies and standard deviations are represented in terms of %.

Descriptor	Direct	$K = 1$	$K = 5$	$K = 10$	$K = 20$	$K = 50$
SIFT	83.62±1.34	73.63±2.90	85.28±2.21	85.20±2.55	84.73±2.53	81.95±3.30
HOG	83.43±2.91	81.85±1.82	90.62±1.73	91.53±2.09	92.62±2.13	91.77±2.92
LBP	90.00±0.85	84.72±3.14	92.38±2.40	93.72±1.73	93.57±2.22	91.45±2.58

Table 4. Face verification results using sparse association with embedding. Mean accuracies and standard deviations are represented in terms of %.

Descriptor	Direct	no embedding	embedding (p=50)	embedding (p=100)
SIFT	83.62±1.34	93.30±1.67	94.20±2.87	94.17±2.86
HOG	83.43±2.91	91.77±2.01	96.33±2.20	95.97±2.13
LBP	90.00±0.85	94.82±1.84	96.40±2.00	96.47±1.94

which were set to the SVM scores. The regularization parameter λ in Equation (5) was set to 0.01. Table 1 shows the face verification results based on a K-NN association without embedding. The number of nearest identities, K, varied from 1 to 50, and the highest performance was obtained for $K = 20$. The verification performance using a sparse association without embedding is shown in the third column of Table 4. Figure 6 shows the ROC curves with varying values of K, and Figure 7 provides the ROC curves of three low-level descriptors. Experimental results without embedding show that sparse association outperforms K-NN association.

Prediction Comparison The face verification results of a K-NN association with embedding are shown in Tables 2 and 3. The dimensionality of the embedding space was set to 50 or 100. In Table 4, the last two columns show the effect of the dimensionality of the embedding space with a sparse association. The ROC curves of both association methods with and without the use of embedding are in Figure 9, and the effect of the dimensionality of the embedding space is shown in Figure 8. We can easily see that the embedding significantly improves the verification performance. Our best performance was achieved when using both sparse association and embedding.

5 Conclusion

Motivated by the AP model, this paper proposed the SSE for face verification. In the association step of the SSE, the sparse representation was used to obtain the reconstructive weight vector. In the prediction step of the SSE, sparsity shared embedding vectors that preserve all of the inter-personal structures were then obtained. Finally, the predictions of the inputs under a shared embedding space

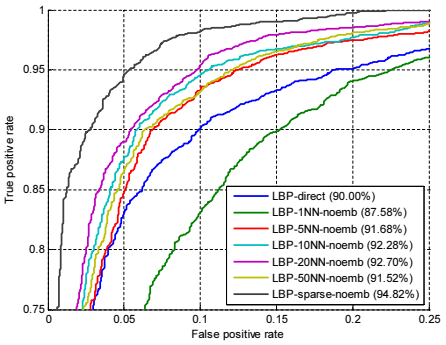

Fig. 6. ROC curves of K-NN association with varying K and sparse association without embedding.

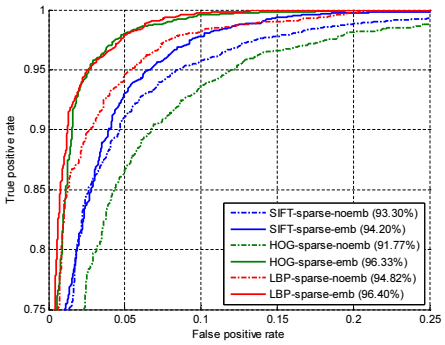

Fig. 7. ROC curves of 3 low-level descriptors using sparse association with/without embedding.

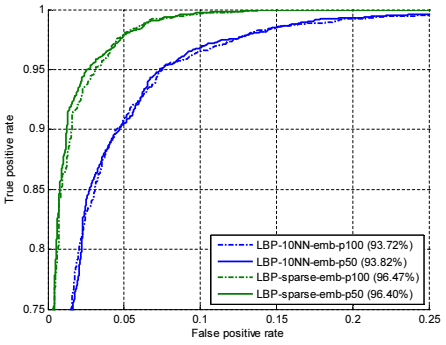

Fig. 8. ROC curves of K-NN association and sparse association with varying dimensionality of the embedding space.

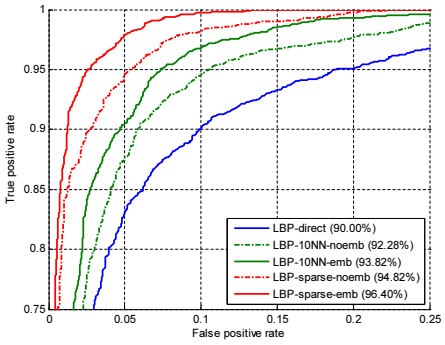

Fig. 9. ROC curves of K-NN association and sparse association with/without embedding.

were used for verification. The experimental results on the MultiPIE dataset showed that the SSE method performs better than the AP model in terms of the verification rate. However, the SSE method is limited when the intra-personal setting of test data does not exist in identity dataset, and we consider to apply the SSE method to this case as future works.

Acknowledgement. This work was supported by the National Research Foundation of Korea (NRF) grant funded by the Korea government (MEST) (No.2012-0005378 and No.2012-0000985).

References

1. Blanz, V., Vetter, T.: Face recognition based on fitting a 3d morphable model. IEEE Transactions on Pattern Analysis and Machine Intelligence **25** (2003) 1063–1074
2. Cao, X. and Wei, Y. and Wen, F., Sun, J.: Face alignment by explicit shape regression. In: Computer Vision and Pattern Recognition. (2012)
3. Chang, C., Lin, C.: Libsvm: a library for support vector machines. ACM Transactions on Intelligent Systems and Technology (TIST) **2** (2011) 27
4. Dalal, N., Triggs, B.: Histograms of oriented gradients for human detection. In: Computer Vision and Pattern Recognition. (2005)
5. Guillaumin, M., Verbeek, J., Schmid, C.: Is that you? metric learning approaches for face identification. In: International Conference on Computer Vision. (2009)
6. He, X., Cai, D., Yan, S., Zhang, H.: Neighborhood preserving embedding. In: International Conference on Computer Vision. (2005)
7. He, X., Yan, S., Hu, Y., Niyogi, P., Zhang, H.: Face recognition using laplacianfaces. IEEE Transactions on Pattern Analysis and Machine Intelligence **27** (2005) 328–340
8. Kumar, N., Berg, A., Belhumeur, P., Nayar, S.: Attribute and simile classifiers for face verification. In: International Conference on Computer Vision. (2009)
9. Lowe, D.: Distinctive image features from scale-invariant keypoints. International Journal of Computer Vision **60** (2004) 91–110
10. Nguyen, H., Bai, L.: Cosine similarity metric learning for face verification. In: Asian Converence on Computer Vision (2011)
11. Niyogi, X.: Locality preserving projections. In: Advances in Neural Information Processing System. (2004)
12. Ojala, T., Pietikainen, M., Maenpaa, T.: Multiresolution gray-scale and rotation invariant texture classification with local binary patterns. IEEE Transactions on Pattern Analysis and Machine Intelligence **24** (2002) 971–987
13. Qiao, L., Chen, S., Tan, X.: Sparsity preserving projections with applications to face recognition. Pattern Recognition **43** (2010) 331–341
14. Roweis, S.T., Saul, L.K.: Nonlinear dimensionality reduction by locally linear embedding. Science. **290** (2000) 2323–2326
15. Schroff, F., Treibitz, T., Kriegman, D., Belongie, S.: Pose, illumination and expression invariant pairwise face-similarity measure via doppelgänger list comparison. In: International Conference on Computer Vision. (2011)
16. Su, Y., Shan, S., Chen, X., Gao, W.: Adaptive generic learning for face recognition from a single sample per person. In: Computer Vision and Pattern Recognition. (2010)
17. Tang, X., Wang, X.: Face sketch recognition. IEEE Transactions on Circuits and Systems for Video Technology **14** (2004) 50–57
18. Wolf, L., Hassner, T., Taigman, Y.: Similarity scores based on background samples. In: Asian Converence on Computer Vision (2010)
19. Wright, J., Yang, A., Ganesh, A., Sastry, S., Ma, Y.: Robust face recognition via sparse representation. IEEE Transactions on Pattern Analysis and Machine Intelligence **31** (2009) 210–227
20. Yin, Q., Tang, X., Sun, J.: An associate-predict model for face recognition. In: Computer Vision and Pattern Recognition. (2011)